

Full Articles

Fragmentation of valine and proline in resonant free electron capture reactions

M. V. Muftakhov and P. V. Shchukin*

*Institute of Molecule and Crystal Physics, Ufa Research Center of the Russian Academy of Sciences,
151 prosp. Oktyabrya, 450075 Ufa, Russian Federation.
Fax: +7 (347) 235 9522. E-mail: LMSNI@anrb.ru*

The processes of resonant electron capture by molecules of valine and proline were studied. The main dissociative decay channels of molecular ions and the structures of fragment ions were established. The reactions of simple bond cleavage and H-shift rearrangement processes were revealed. The dissociative electron attachment cross-sections for $[M - H]^-$ ions were measured in the region of 1.25 eV. The metastable decay of $[M - H]^-$ ions were found in the energy region of 4.5–8 eV. The structures of decomposing parent ions were determined using the statistical model of metastable fragmentation.

Key words: dissociative electron attachment, negative ions, metastable ions, valine, proline.

Considerable attention is given presently to processes of resonant electron capture by biologically significant compounds (amino acids, nucleosides, vitamins, *etc.*) and related objects. It is especially interesting to study the processes of formation and decay of negative ions of amino acids, being building blocks of protein macromolecules, which play the key role in processes of living activity of organisms. The processes of resonant electron capture by molecules of some aliphatic,^{1–7} aromatic,⁷ and heterocyclic^{7–10} amino acids have been studied to date. As a result, the mechanisms of attachment of extra-electrons were established and the main decay channels of molecular negative ions were revealed. At the same time, the obtained results put new questions about mechanisms of molecular ion decay and the structures of the fragment ions formed. The present work is devoted to the study of processes of resonant energy-controlled electron capture

by valine (Val) and proline (Pro) molecules. These amino acids have close atomic composition but different structures: branched and cyclic, respectively. Therefore, the combined study of these objects should reveal specific features of the influence of the molecular structure on the processes of ion formation and favor to identify fragment ions.

Experimental

Experiments were carried out on a MI-1201V magnetic mass spectrometer modified for studying both positive and negative ions.¹¹ Switching between detection modes for different ions was carried out by a change in the polarity on the electrodes of the ion-optical systems and analyzing electromagnet. The electron beam emitted from the cathode interacts with vapors of the studied compound in the ionization chamber. Negative ions formed due to dissociative electron attachment processes are withdrawn from the ionization region, focused, accelerated, se-

lected by masses in the magnetic analyzer, and detected by a secondary electron multiplier. The electron beam energy is specified by a computer into which the detected ionic signal is put synchronously. A specific feature of the device is the possibility to study processes of autodetachment of electrons. For this purpose, an additional electrode was mounted in the detection system. This electrode makes it possible to deviate the charged component of the ion beam in the transverse electric field and to detect the flow of neutral particles (neutrals) formed due to spontaneous ejection of captured electrons by the ions during their drift in the second field-free area of the spectrometer.

Valine and proline were purchased from Sigma/Aldrich Chemical Co. Effective yield curves of ions were recorded at $T \approx 100^\circ\text{C}$ and the energy electron distribution at the half-height $\Delta E_{1/2} \approx 0.5$ eV. Experiments on studying metastable decays were carried out at $T \approx 116^\circ\text{C}$ and $\Delta E_{1/2} \approx 0.4$ eV. The electron energy scale was calibrated by maxima of the resonance peaks $\text{SF}_6^-/\text{SF}_6$ (~ 0 eV) and $[\text{M} - \text{H}]^-/\text{MeCOOH}$ (~ 1.55 eV).¹² The appearance energy of ions $\text{SF}_6^-/\text{SF}_6$ (~ 0 eV) was used as a zero mark when determining threshold energies of dissociative reactions. The experiments were carried out with mass resolution $R \approx 1000$, and in the case of separation of isobaric ions, the resolution of the device was increased to $R \approx 2000$. Since the peak of metastable ions is broader than those of normal ions, the effective yield curves of metastable ions were recorded with widely open gaps of the detection system in order to completely take into account the number of metastable ions. The cross-section of dissociative electron attachment for fragment ions was determined by a described procedure.¹³

Calculation procedure

Threshold energies for the reactions of formation of fragment negative ions (AE) were calculated from the standard enthalpies of formation (ΔH_f°) of neutral particles and ions involved in the reactions (Table 1). The values of ΔH_f° were calculated by the density functional method in the B3LYP/6-311+G(3df,2p) basis set with preliminary geometry optimization in the B3LYP/6-311+G(d,p) basis set and final correction of the enthalpy values by the X1 neutron method.¹⁴

The ratios of metastable ions (m^*), product ions (D^-), and precursor ions (P^-) $[m^*]/[P^-]$ and $[D^-]/[P^-]$ were calculated according to the statistical model of metastable fragmentation.¹⁵ These ratios were calculated from the function of ion distribution by the internal energy $f(E)$ and microcanonical decay rate constant $k(E)$. The ion distribution $f(E)$ was simulated by the Gaussian function with several parameters, whereas the microcanonical rate constants of metastable decays were calculated using the Rice—Ramsperger—Kassel—Marcus (RRKM) theory¹⁶ according to the equation

$$k = \frac{\sigma W^\pm(\epsilon - E_a)}{h\rho(\epsilon)},$$

where ϵ is the internal energy of ions, σ is the coefficient of reaction route degeneration, $W^\pm(\epsilon - E_a)$ is the sum of states in the activated complex in the energy interval from zero to $(\epsilon - E_a)$, E_a is the activation energy, h is Planck's constant, and $\rho(\epsilon)$ is the density of states in an active molecule.

The vibrational frequencies of decomposing precursor ions calculated by the B3LYP/6-311+G(d,p) method were used for the calculation of the functions $\rho(\epsilon)$ and W^\pm . In the case of W^\pm , the vibration mode corresponding to the vibration of the cleaved bond was excluded from the calculation. The activation energies (E_a) of dissociative reactions were accepted to be equal to the difference between the calculated threshold appearance energies of product ions and precursor ions assuming that the barrier of the backward reaction was absent.

Results and Discussion

Resonant electron capture by valine and proline molecules occurs in the energy range from 0 to 12 eV and results in the formation of many fragment negative ions, whose effective yield curves (EYC) as functions of the energy of captured electrons are presented in Figs 1 and 2, respectively. The processes of formation of negative ions in these compounds have been studied earlier.^{3,4,8–9}

Ions $[\text{M} - \text{H}]^-$. The $[\text{M} - \text{H}]^-$ ions formed in a region of 1.25 eV are predominant ions in the mass spectra of Val

Table 1. Calculated enthalpies of formation of neutral particles and ions (ΔH_f°)

Ion/neutral particle	$\Delta H_f^\circ/\text{eV}$	Ion/neutral particle	$\Delta H_f^\circ/\text{eV}$
Val	−4.74	$\text{CH}_2\text{CH}_2\text{CH}_2\text{COO}^-$	−3.65
Pro	−3.72	NH_2	1.85
$\text{Me}_2\text{CHCH}_2\text{COO}^-$	−5.99	NH_3	−0.50
$\text{Me}_2\text{CHCHCOO}^-$	−4.13	HCOOH	−3.93
$\text{CH}_2=\text{CHCH}_2\text{CH}_2\text{COO}^-$	−4.71	$\text{NHCH}(\text{CHMe}_2)\text{COOH}^-$	−3.96
$\text{CH}_2=\text{CHCH}_2\text{CHCOO}^-$	−2.92	$\text{NH}_2\text{C}(\text{CHMe}_2)\text{COOH}^-$	−4.60
$\text{NHCH}=\text{CMe}_2^-$	0.47	NHCHCHMe_2	0.01
$\text{NH}=\text{CCHMe}_2^-$	1.39	COOH^-	−3.40
$\text{NH}_2\text{C}=\text{CMe}_2^-$	1.62	COOH	−1.89
$[\text{cyclo}-(\text{NCH}_2\text{CH}_2\text{CH}_2\text{CH}_2)]^-$	1.16	$\text{NH}_2\text{CH}(\text{CMe}_2)\text{COOH}^-$	−3.53
$\text{H}_2\text{C}=\text{CHCOO}^-$	−4.24	$\text{NH}_2\text{CHCMe}_2$	−0.05
$\text{CH}_2\text{CH}_2\text{NH}_2$	1.57	$\text{NH}_2\text{CH}(\text{CHMe}_2)\text{COO}^-$	−5.83
$\text{CH}_3\text{CH}=\text{CHCOO}^-$	−4.55	HCOO^-	−5.06
NH_2CH_2	1.43	CO_2	−4.22
$\text{NH}=\text{CH}_2$	0.90	H	2.29

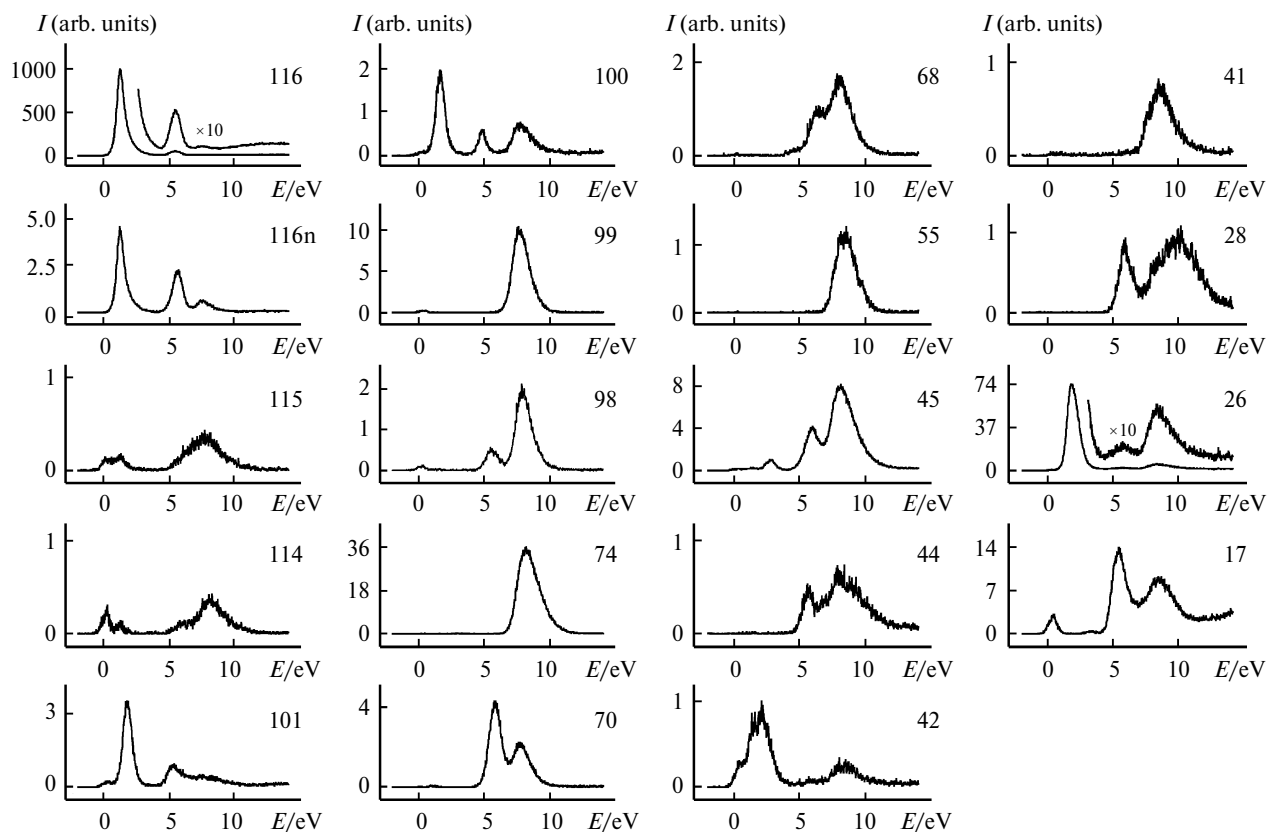


Fig. 1. Effective yield curves for negative ions from valine. Here and in Fig. 2, the mass number (m/z) of ions is given at upper right; E is the energy of electrons, and I is the intensity.

and Pro. This highly efficient decay channel is characteristic of the previously studied organic acids^{17–19} and amino acids^{1–10} and is related to the elimination of the H atom of the carboxyl group. The measured cross-section of dissociative electron attachment (DEA) for these ions is $7.6 \cdot 10^{-19} \text{ cm}^2$ for Val and $2.9 \cdot 10^{-19} \text{ cm}^2$ for Pro. The latter agrees well with the value of $2.9 \cdot 10^{-19} \text{ cm}^2$ obtained²⁰ for Pro. As can be seen, the DEA cross-section of the $[M - H]^-$ ions is several times lower than that in valine. One of the reasons for this difference can be due to a more compact structure of the molecule. As a result, the electron is captured by the Pro molecule with a smaller cross-section than Val, which, in turn, reflects the cross-section of formation of fragment ions. However, in spite of relatively small sizes of the molecules, the cross-section for glycine and alanine is $\sigma_{[M-H]^-} = 4.5 \cdot 10^{-19}$ and $5.6 \cdot 10^{-19} \text{ cm}^2$, respectively, which is close to the analogous value for valine. Note that these values of cross-sections differ from previously²¹ obtained values of $1.3 \cdot 10^{-18} \text{ cm}^2$ (glycine) and $1.6 \cdot 10^{-18} \text{ cm}^2$ (alanine), which were estimated less correctly. Another reason for the difference in the cross-sections of formations of the $[M - H]^-$ ions in Val and Pro can be a specific feature of the mechanism of formation of the discussed ions. In amino acids the $[M - H]^-$ ions at 1.3 eV are formed by the decomposi-

tion of the dipole-bound state of molecular ions.²² This process occurs only in one of the conformers with a higher dipole moment. The $[M - H]^-$ ions from Val and Pro at 1.25 eV are generated, most likely, *via* a similar mechanism. However, in the case of proline, the mole fraction of the conformer with the higher dipole moment is probably small, which decreases the yield of the $[M - H]^-$ ions.

As can be seen from Figs 1 and 2, the low-energy resonance peak in the EYC of the $[M - H]^-$ ions has a smooth right slope, indicating the possibility of the presence of another resonance state. Probably, this is the resonance of the form with the capture of an electron to the vacant molecular orbital π_{00}^* , which is observed in the spectra of passing electrons at 1.91 eV.²⁰ One more resonance peak prevails in the region of medium EYC energies of the $[M - H]^-$ ions in Val and Pro. As in the case of glycine,⁷ the mechanism of electron capture in this resonance state is probably associated with the electron-excited Feshbach resonance, whose parent state can be the singlet-excited state $n-\pi^*$ or the Rydberg state $n-3s$. The low-intensity peak is observed at 7.5 eV in the EYC of the $[M - H]^-$ ions against the background of secondary processes. For its identification, we recorded the effective yield curves for neutral particles $[M - H]^0$ formed due to the autodetach-

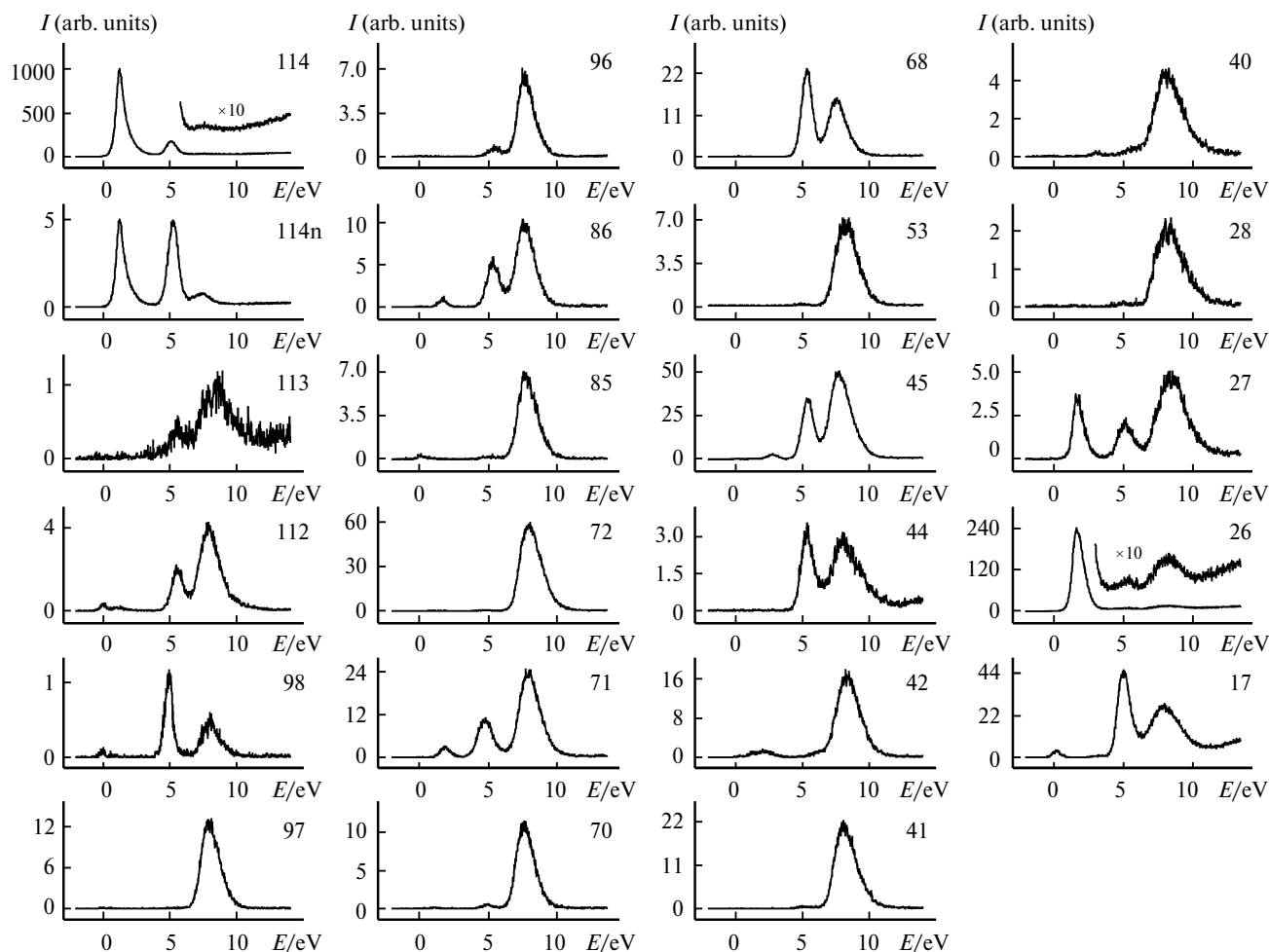


Fig. 2. Effective yield curves for negative ions from proline.

ment of electrons by the $[M - H]^-$ ions in the field-free area of the spectrometer (designed as 116n and 114n in Figs 1 and 2, respectively). Unlike of the EYC of ions, the curves of neutral particles contain almost no background from secondary processes, which makes it possible to detect low-intensity resonance states. As can be seen from Figs 1 and 2, the curves of $[M - H]^0$ in valine and proline demonstrate three resonance peaks. In the low-energy region, they are formed due to the collision of ions with molecules of the residual gas, because here ions are formed near the threshold. At the same time, in the energy region higher than 4 eV, the shape and maxima of the peaks of ions and neutrals differ, which indicates the occurrence of spontaneous electron ejections and confirms the formation of the long-lived ions $[M - H]^-$ in the region of 7.5 eV. Note that the ratio of neutral particles and ions from which they are generated, $[M - H]^0/[M - H]^-$, reflects the efficiency of the autoneutralization process. The $[M - H]^0/[M - H]^-$ curves as functions of the electron energy obtained for Val and Pro differ slightly. This fact indicates that in both objects the processes of electron

autodetachment in the energy range from 4 to 8 eV occur with nearly equal efficiency and, hence, the molecular structure exerts almost no effect on the autoneutralization of the $[M - H]^-$ ions under other equivalent conditions.

Ions formed by the detachment of the N- and C-terminal fragments. We considered dissociative processes in glycine, alanine, and valine resulting in the formation of fragment ions $[M - 16]^-$, $[M - 17]^-$, $[M - 18]^-$, and $[M - 19]^-$.²³ These ions are formed due to the elimination of the N- and C-terminal groups responsible for the formation of peptide groups. It was found that the $[M - 16]^-$ and $[M - 19]^-$ ions corresponded to the ions with the elemental composition $[M - NH_2]^-$ and $[M - H - H_2O]^-$ formed in two energy regions. Experiments on the precise measurement of ion masses revealed no negative ions with different stoichiometry. These ions served as internal calibrants for the identification for the $[M - 17]^-$ and $[M - 18]^-$ ions. The precise measurement of the mass showed that the former corresponded to the structures $[M - NH_3]^-$ at low energies (1–2 eV) and $[M - OH]^-$ at

high energies (5 eV). The latter are formed by the ejection of the nitrogen atom and four hydrogen atoms in various combinations. It follows from the published data²³ that at 1.8 eV the ions m/z 101 and 100 in Val are associated with ions of the $[M - \text{NH}_2]^-$ and $[M - \text{NH}_3]^-$ type, respectively, and are formed in the rearrangement reactions



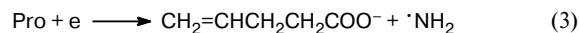
($AE = 0.6$ eV),



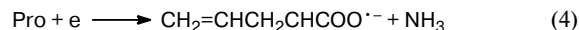
($AE = 0.11$ eV).

No $[M - 16]^-$ ions were detected in the mass spectra of proline obtained with high mass resolution at fixed energies of 1.8, 5.0, and 7.9 eV (Fig. 3, *a*). The peak of the $[M - 17]^-$ ions with m/z 98 was detected only at 5 eV, and the elemental composition $[M - \text{OH}]^-$ corresponds to this peak. In the region of 8 eV, the peak with the nominal mass m/z 98 is an isotopic peak of the $[M - 18]^-$ ions with m/z 97. Thus, in the reactions of electron capture by the Pro molecules, the $[M - \text{NH}_2]^-$ and $[M - \text{NH}_3]^-$ ions are

not formed but, nevertheless, the calculations indicate the possibility of H-shift reactions



($AE = 0.86$ eV),



($AE = 0.3$ eV).

Therefore, the energy factor is not an obstacle in this case, and the absence of the ions discussed can be explained by other factors: competition from the process of electron autodetachment in the long-lived molecular ion or the cyclic structure of the proline molecule. However, the ions with m/z 86 and 71 observed in the region of lower energies have explicitly rearrangement origin and prejudice the hypothesis about the exclusive role of the time factor. It is most likely that time exerts an indirect influence and the main reason is the cyclic structure of the proline molecule contrary to that of valine. In fact, since the nitrogen atom is included into the cycle and is bonded with two carbon atoms, there is no NH_2 fragment necessary for elimination. Therefore, the occurrence of hypo-

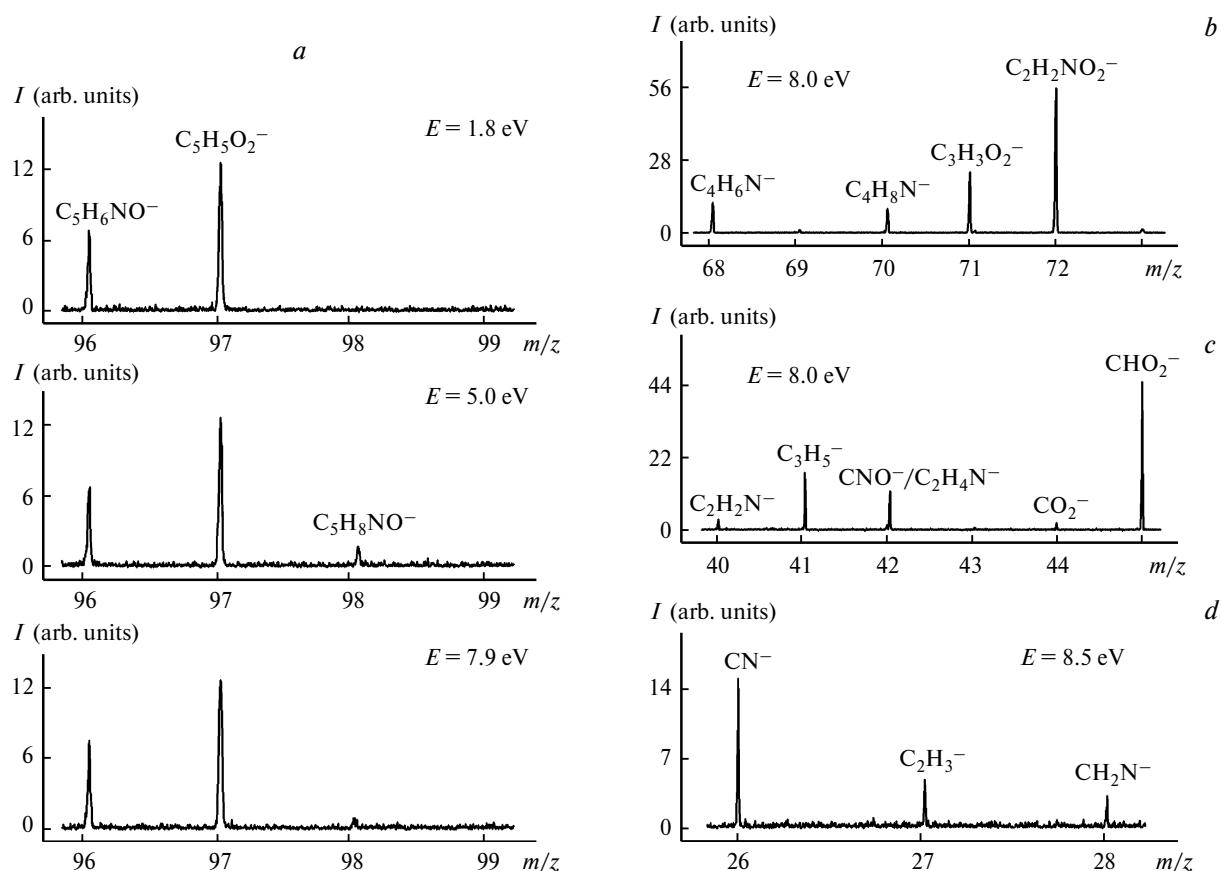


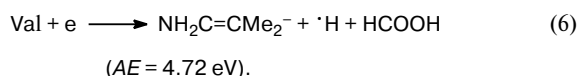
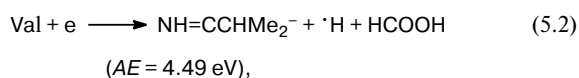
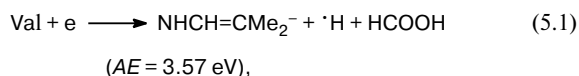
Fig. 3. Fragments of the mass spectra of negative ions from proline recorded at fixed energies of electrons (E) with high mass resolution.

thetical reaction (3) in Pro compared to reaction (1) in Val should be accompanied by additional H-shift processes in the molecular ion.

It should be mentioned that the $[M - 18]^-$ ions ($[M - 2H - NH_2]^-$ or $[M - H - H_2 - NH]^-$) also formed due to the decomposition of the N-terminal fragment are probably generated due to the consecutive decay of the M^- ions through the intermediate $[M - H]^-$ ions. In this case, the H-shift occur in the long-lived fragment ion and the influence of the time factor is low.

The reactions of formation of the $[M - OH]^-$ and $[M - H - H_2O]^-$ ions in valine and proline are identical and have earlier been discussed in detail for valine.²¹ It should be mentioned here that the low yield of the $[M - OH]^-$ ions is caused, most likely, by the competition from the formation of OH^- upon the simple C—O bond cleavage.

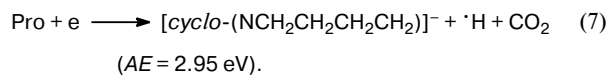
Ions of medium masses. It is most likely that the ions with m/z 55 in Val and m/z 53 in Pro are analogs to the $CH_2=CH^-$ ions in alanine²¹ and have the structures of the vinyl anions $Me_2C=CH^-$ and $CH_2=CHCH=CH^-$. Since they are formed at high energies, the determination of the neutral product in the reactions of their formation is ambiguous. The resemblance of the effective yield curves of the ions with m/z 68 in Pro and m/z 70 in Val suggest that they are of one type and represent the $[M - H - CH_2O_2]^-$ ions. In Val three structures formed in the following rearrangement reactions satisfy the experimental appearance energy of these ions $AE_{exp} = 5.24$ eV:



Another pair of the single-type ions with m/z 72 in Pro and m/z 74 in Val detected in the high-energy is represented by the $[M - C_3H_7]^-$ ions. In the case of Val, they are formed by the detachment of the alkyl substituent at the C_α atom by the simple bond cleavage as in leucine and isoleucine.⁵ The Pro molecule contains no lateral fragment C_3H_7 , and the $[M - C_3H_7]^-$ ions can be formed only due to the H-shift in the molecular ion, which is poorly probable because of the time factor. We assume that this is consecutive fragmentation through the intermediate $[M - H]^-$ ion.

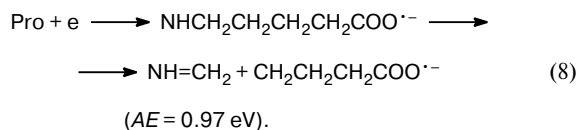
The experiment with high mass resolution made it possible to identify in Pro the elemental composition of ions m/z 70 and 71 as $[M - CHO_2]^-$ and $[M - C_2H_6N]^-$, respectively (Fig. 3, *b*). The peaks of ions with m/z 68 ($C_4H_6N^-$) and m/z 72 ($C_2H_2NO_2^-$) were used as internal calibrants. Concerning the ions with m/z 70, it is a natural

assumption about their formation in the simple cleavage of the R—COOH bond. However, alkyl radicals, except for $\cdot\text{Me}$ (electron affinity $EA = 0.08$ eV),²⁴ are characterized by the negative value of EA , which shows that the discussed ions have another structure and are formed due to rearrangement. Possibly, ions with the cyclic structure with the "localized" additional electron on the nitrogen atom are generated



There are no hindrances for an analogous process with migration of the H atom of the NH_2 group to the C_α atom in valine and in leucine and isoleucine; however, no $[M - 45]^-$ ions were detected in the mass spectra of the listed compounds.⁵ Therefore, in Pro the $[M - 45]^-$ ions are formed *via* the mechanism inaccessible for amino acids of the noncyclic structure.

As mentioned above, the cyclic structure of the proline molecule results in the absence in its spectrum of the $[M - NH_2]^-$ and $[M - NH_3]^-$ ions, which are detected in Val and other amino acids with the branched structure. At the same time, the channels of formation of these ions in Pro are transformed during the isolation of fragment $[M - CH_3N]^-$ (m/z 86) and $[M - C_2H_6N]^-$ (m/z 71) ions. Here, unlike amino acids with the branched structure, the C_α —N bond cleavage results not in molecular ion fragmentation but in its isomerization accompanied by ring opening. As for the formation of the $[M - NH_2]^-$ and $[M - NH_3]^-$ ions in Val, the necessary conditions for these reactions to occur is the presence of hydrogen bonds in decaying precursor ions. This rearrangement process occurs *via* the following scenario. The attachment of the low-energy electron results in the O—H bond cleavage, due to which the H atom is retained in the composition of the molecular ion by the weak hydrogen bond. The subsequent C_α —N bond cleavage results in the formation of two radical centers: on the nitrogen and carbon atoms, which compete for the possibility to attach the isolated H atom. In the case of its migration to the carbon atom, the molecular ion of Pro is isomerized to the structure $NHCH_2CH_2CH_2CH_2COO^{\cdot-}$. The decomposition of this ion can proceed only *via* the channels accessible from the viewpoint of the energy and time factors. The reaction of simple C—C cleavage with the formation of $[M - CH_3N]^-$ (m/z 86) ions

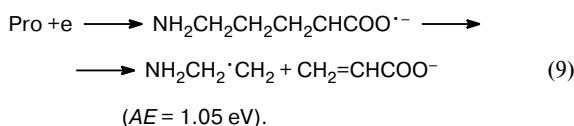


satisfies this condition.

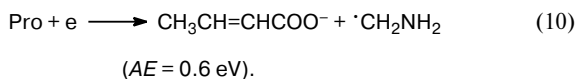
Note that in peptides the intramolecular hydrogen bond is stronger due to the interaction of the carboxylic H atom

not with a particular N atom but with the whole peptide moiety. Therefore, in a similar reaction after the cleavage of the C_α —N bond, an isolated H atom remains with the nitrogen atom, resulting in a substantially higher efficiency of formation of the analog of the $[M - NH_3]^-$ ions compared to the formation of the analog of the $[M - NH_2]^-$ ions in the low-energy region.²¹

In the case of the attachment of the carboxylic hydrogen atom to the nitrogen followed by pyrrolidine ring opening, the molecular ion is transformed into the $NH_2CH_2CH_2CH_2CHCOO^{\cdot-}$ structure. The further fragmentation of this ion is related to the C—C bond cleavage and formation of the fragment ion $[M - C_2H_6N]^-$ (m/z 71)



The decomposition of the isomerized $[M]^-$ ion via other channels is poorly efficient. The simple cleavage of the N—C bond to form $CH_2CH_2CH_2CHCOO^-$ and $\cdot NH_2$ moieties is energetically impossible, as well as the simple C—C bond cleavage with the formation of the $CH_2CH_2CHCOO^-$ and $\cdot CH_2NH_2$ moieties (ions with m/z 85). The H-shift reactions (3) and (10) leading to fragments with a low enthalpy of formation are suppressed by the time factor, as well as rearrangement reaction (4) with the formation of the $[M - NH_3]^-$ ions

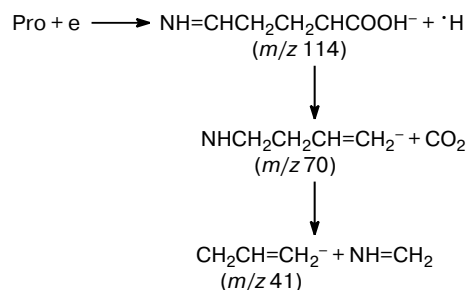


In the region of high energies, the ions with m/z 71 and 86 (as well as those with m/z 85) in Pro are formed with the intermediate $[M - H]^-$ ions, but the order of dissociation of certain bonds is likely retained in the course of these reactions as in the low-energy region. Namely, the O—H bond is cleaved first with H atom elimination, then the C_α —N bond dissociates with ring opening, etc.

Since there are no appropriate reference peaks, it was impossible to experimentally identify the elemental composition of the ions with m/z 85 in Pro. It is most likely that they correspond to the $[M - CH_4N]^-$ ions having the filled electronic shell rather than to the $[M - C_2H_6]^\cdot$ radical ions. As in the case of the ions with m/z 71, the possibility of formation of the ions with m/z 85 ($[M - CH_4N]^-$) in Pro is caused by the existence of the CH_2NH moiety in the structure of the molecule. At the energy > 4 eV we assume the consecutive decay through the intermediate $[M - H]^-$ ions. In the low-energy region, no ions with m/z 85 were detected, although the energy factor does not prevent process (10) to occur.

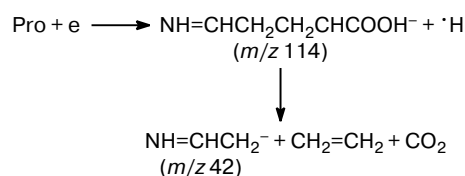
Ions with small masses. Some aspects of formation of ions with small masses from amino acids were discussed in earlier studies. In particular, it was assumed⁷ that in gly-

cine and alanine the elemental compositions CHO_2^- and CO_2^- correspond to the ions with m/z 45 and 44, whereas for the ions with m/z 42 compositions $C_2H_4N^-$, $C_2H_2O^-$, and CNO^- are possible. In order to identify the elemental composition of the listed negative ions in Pro, we carried out an experiment with high mass resolution. Figure 3 presents the fragment of the mass spectrum of Pro at 40–45 amu recorded at an energy of 8 eV. The CHO_2^- (m/z 45) and $C_3H_5^-$ (m/z 41) ions were used as internal calibrants. It should be mentioned that in glycine and alanine the ions with m/z 41 have the C_2HO^- structure,²¹ and hence, we expected an analogous interpretation for proline. However, as shown by the detailed analysis of the mass spectra, the ions with m/z 41 in Pro are associated with the $C_3H_5^-$ type. The formation of these ions probably proceeds via the following mechanism. The negative molecular ion of proline ejects the carboxylic H atom and is isomerized to the linear $[M - H]^-$ ion; the C_α — CO_2 bond dissociation in the $[M - H]^-$ ion is accompanied by the migration of the H atom with the formation of the ion with m/z 70; the latter, in turn, gives the ion with m/z 41 due to the simple cleavage of the C—C bond.

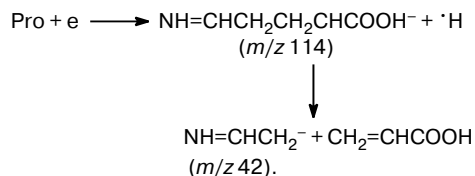


The ions with m/z 45 in the low-energy region have the structure of $HCOO^-$ and are the product of the H-shift reaction. In the energy region > 4 eV, they are predominantly formed by the simple C— C_α bond cleavage and the $COOH^-$ structure. The ions with m/z 42 are identified as $C_2H_4N^-$ with a small contribution of the CNO^- ions.

The mechanism of formation of the intense ions with m/z 42 ($C_2H_4N^-$) in Pro, which are not characteristic of Val, differs slightly, most likely, from that considered above for the ions with m/z 41. We believe that after carboxylic H atom elimination from the M^- ion the C_α —N bond cleavage in the $[M - H]^-$ ion is accompanied by the migration of the H atom from the CH_2 group adjacent to nitrogen to the C_α atom. Then the isomerized $[M - H]^-$ ion, whose structure differs from that considered above, decomposes with the simple cleavage of two C—C bonds.



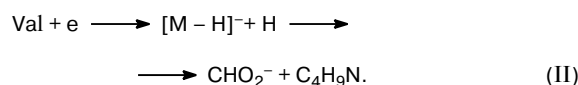
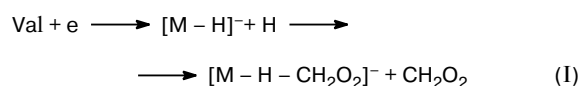
However, the possibility of formation of the $C_3H_5^-$ (m/z 41) and $C_2H_4N^-$ (m/z 42) ions cannot be excluded for other reactions of consecutive decomposition of the M^- ion, whose first step is the dissociation of the $C_\alpha-H$ or $N-H$ bond, and the uncharged products of these reactions can differ from those presented above. For example, the ion with m/z 42 can also be formed in the following process:



The ions with m/z 44 and 40 were interpreted as CO_2^- and $\text{C}_2\text{H}_2\text{N}^-$, respectively, without admixtures of other isobaric ions. We found the ions with m/z 28 in both compounds, being the CH_2N^- ions. The ion with m/z 27 was detected in Pro, and its elemental composition C_2H_3^- was

identified in an experiment with high resolution (Fig. 3, *d*). The CN^- (m/z 26) and CH_2N^- (m/z 28) ions were used as internal calibrants when recording the mass spectrum in the range 26–28 amu.

Metastable ions. The mass spectrum of valine exhibits two peaks of metastable ions with apparent masses m/z 17.46 and 42.24 (Fig. 4, *a*), which indicate the formation of the CHO_2^- and $[\text{M} - \text{H} - \text{CH}_2\text{O}_2]^-$ ions from the $[\text{M} - \text{H}]^-$ ions in the following reactions:



Similar metastable decays were detected in proline, whose mass spectrum contains fractional mass peaks with

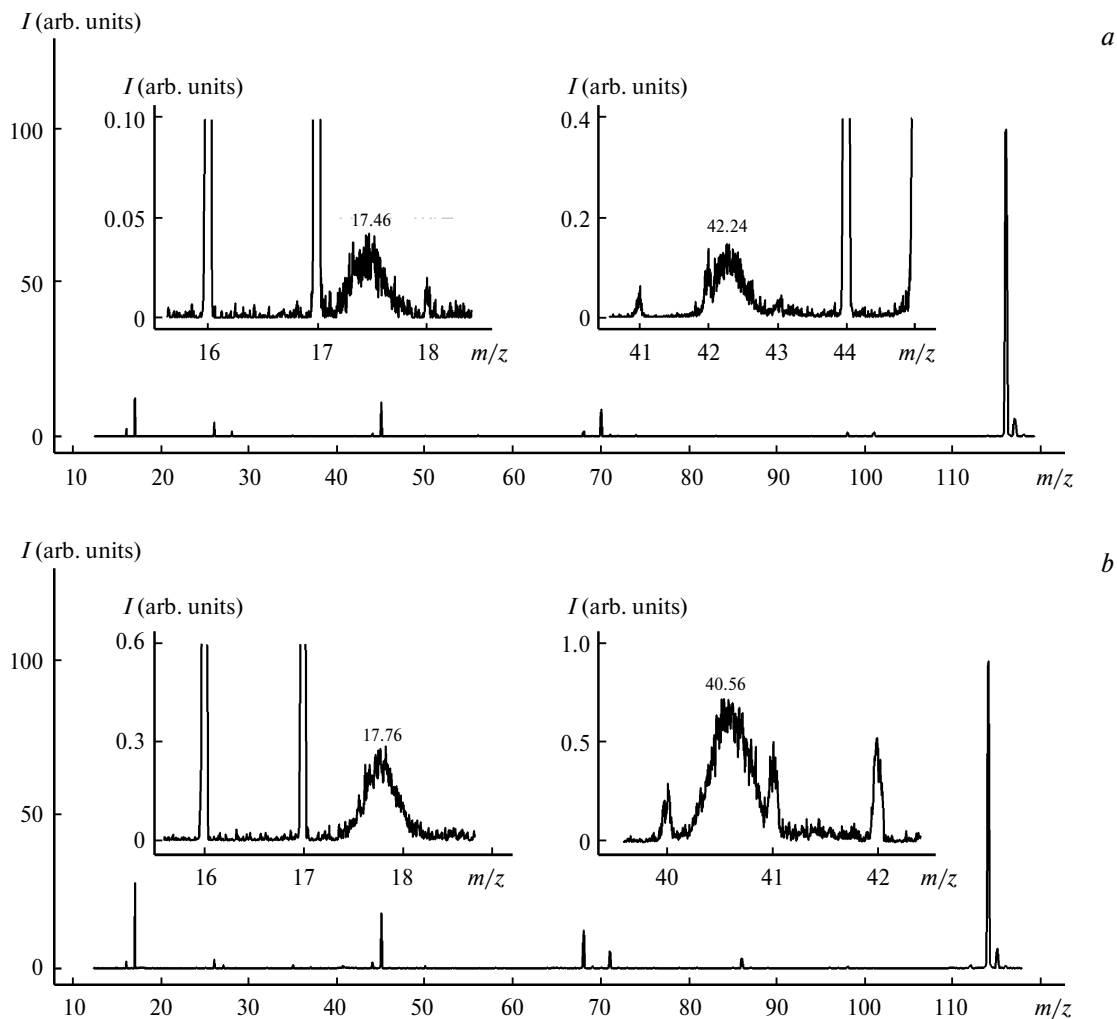


Fig. 4. Mass spectra of negative ions from valine (*a*) and proline (*b*) recorded at an energy of electrons of 5.8 and 5.3 eV, respectively. Insets: the regions of abundance of metastable peaks in an expanded scale.

m/z 17.76 and 40.56 (Fig. 4, *b*). Since these dissociative processes are observed in both amino acids, they are similar. Note that in proline the efficiency of fragmentation is somewhat higher, which can be due to some difference in the energy of the processes and in the spatial structure of the ions.

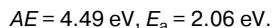
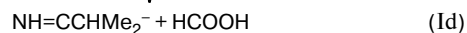
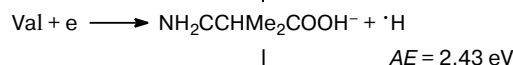
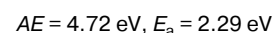
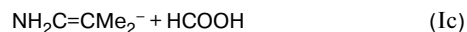
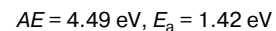
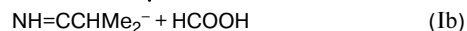
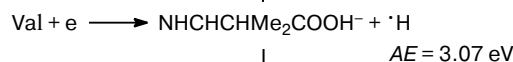
The metastable decays in valine have been observed earlier.²⁵ It was shown that the decaying $[M - H]^-$ ions had the imine structure. The problem of instability of the $[M - H]^-$ ions with respect to the further dissociation was also considered,²⁶ and decays of various types of these ions $[M - H]^-_{-O}$, $[M - H]^-_{-C_\alpha}$, and $[M - H]^-_{-N}$ formed by the elimination of the H atom from the carboxyl group, the C_α carbon atom, and the nitrogen atom, respectively, were simulated.²⁶ The authors of this work also mentioned the possibility of destruction of the imine $[M - H]^-_{-N}$ ions to form the $COOH^-$ ions. At the same time, from the energy point of view, all the three structures of the $[M - H]^-$ ions, whose calculated threshold energies of formation are 1.11, 2.35, and 3.36 eV, respectively, are possible in the medium-energy resonance state in which the considered metastable decomposition was observed. Moreover, it was established⁷ for glycine from experiments with deuterated sample that at 5.5 eV the $[M - H]^-$ ions have the predominantly enolic form, *i.e.*, are formed by the elimination of the hydrogen atom from the C_α carbon atom. Therefore, the question about the structure of the decaying $[M - H]^-$ ions and the mechanism of their fragmentation in the medium-energy region seems interesting.

One of specific features of metastable ions is that they contain information on the energy and structural parameters of decaying ions and on the kinetics of the dissociative process. We earlier used the statistical approach for the description of metastable decay.¹⁵ The model developed in the framework of this approach makes it possible to establish a relationship between the detected yield curves of ions and the calculated values of the decay rate constant and the function of ion distribution over the internal energy. In the present work, we used this statistical model to analyze the metastable fragmentation process of valine in order to establish the decay mechanisms. The model makes it possible to calculate the amount of formed metastable ions and product ions as ratios $[m^*]/[P^-]$ and $[D^-]/[P^-]$, which can be compared with analogous experimental curves.

The effective yield curves of precursor ions (P^-), product ions (D^-), and metastable ions (m^*) for considered decays (I) and (II) in valine are presented in Figs 5, *a* and *b*, respectively. In both cases, the dissociative process covers two resonance states with maxima at 5.7 and 7.8 eV. For analysis of metastable decays, it is more convenient to consider the ratios instead of the EYC themselves, which makes it possible to exclude the resonance nature of formation of negative ions and the influence of experimental factors on the efficiency of the yield of ions. The experimental ratios of the EYC for metastable ions, product ions, and precursor ions in the form of $[m^*]/[P^-]$ and

$[D^-]/[P^-]$ for reactions (I) and (II) are presented in Fig. 6 (solid line). The curves obtained reflect the efficiency of decay at different energies of captured electrons. In the case of the single statistical process, regardless of resonant regions, these curves should represent a monotonically ascending function, as it was observed for the metastable decay in benzyl acridoneacetate.¹⁵ However, as seen from Fig. 6, the curves $[m^*]/[P^-]$ and $[D^-]/[P^-]$ have a break on going from one resonance state to another. A similar character of the curves can be explained as follows. The first explanation is related to the fact that different dissociative processes characterized by different decay rate constants and leading to the formation of fragment ions with different structures occur in the both resonances. The second explanation is that the EYC of the $[M - H]^-$ ions contains a small parasite contribution from secondary process, which results, as can be seen from Fig. 1, in "pulling up" of the yield curve of ions in the high-energy region. As a result, an increase in the intensity of precursor ions P^- decreases the $[m^*]/[P^-]$ and $[D^-]/[P^-]$ ratios with an increase in the electronic energy. It is impossible to unambiguously choose one of the hypotheses without additional studies. Therefore, taking into account the possible violation of the $[m^*]/[P^-]$ and $[D^-]/[P^-]$ curves for the high-energy metastable decay from secondary processes, in this work we analyzed the mechanism of fragmentation of the $[M - H]^-$ ions only in the resonance state at 5.7 eV.

In decay (I) the metastable $[M - H - CH_2O_2]^-$ ions are probably formed due to the elimination of the neutral fragment as a formic acid molecule by the H-shift in the $[M - H]^-$ ions. Taking into account the structure of a valine molecule, this process is most probable for the $[M - H]^-_{-N}$ and $[M - H]^-_{-C_\alpha}$ ions, because in the case of the $[M - H]^-_{-O}$ ion the H-shift requires strong structural changes. The following possible dissociative reactions were considered for this metastable decay:



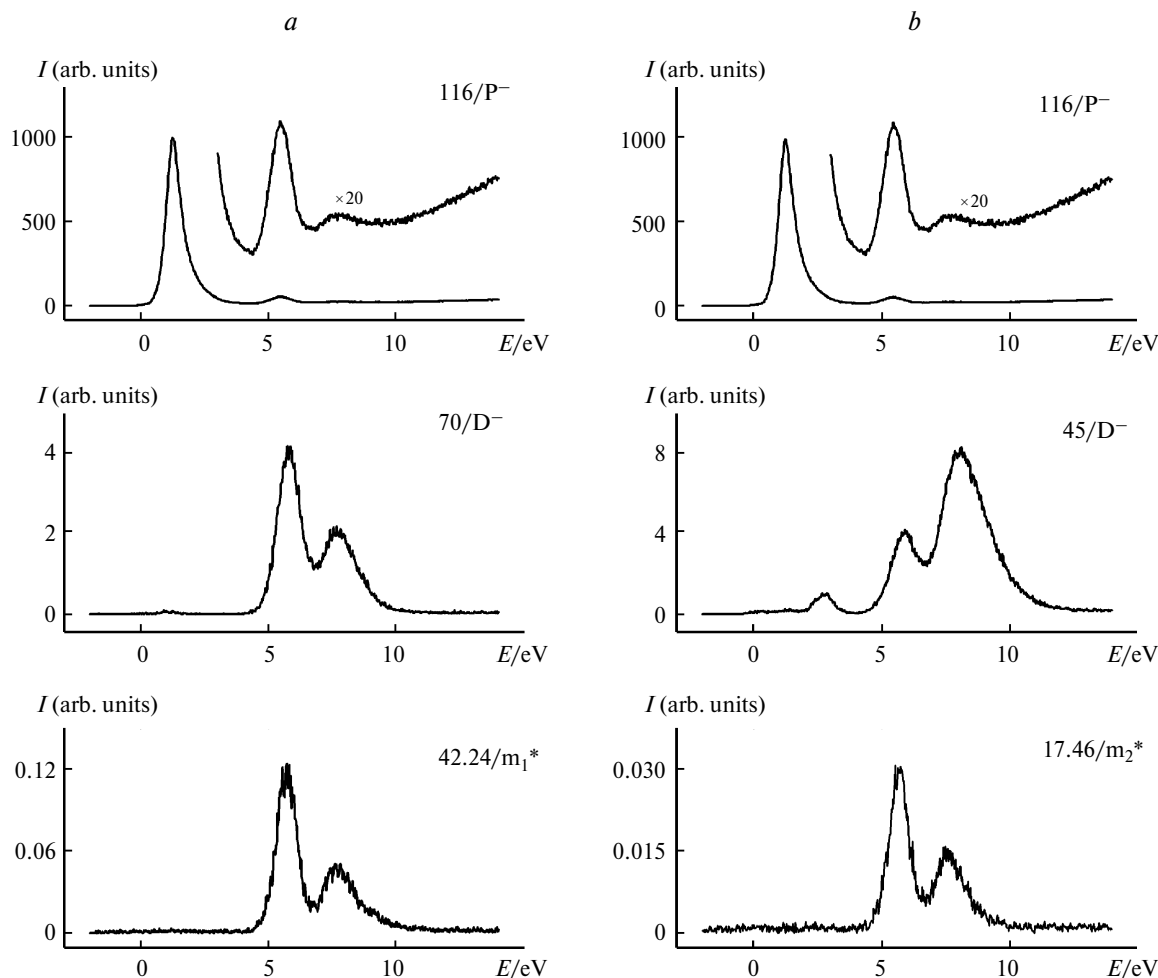
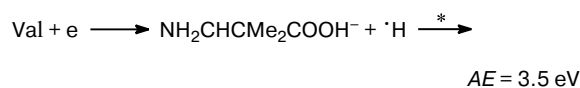
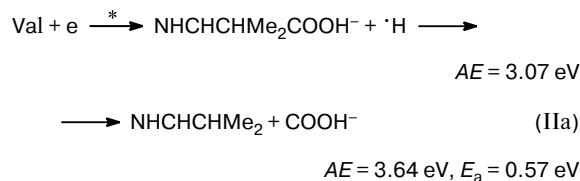


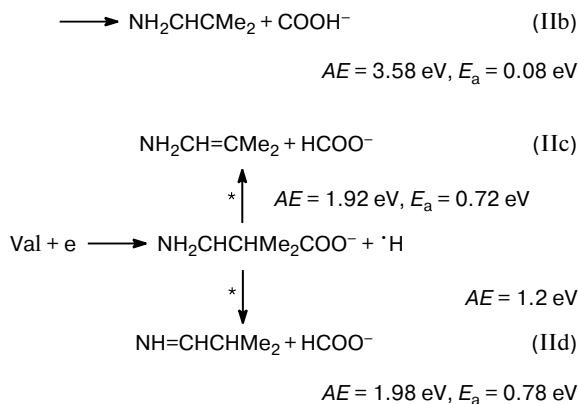
Fig. 5. Effective yield curves of parent ions (P^-), product ions (D^-), and metastable ions (m^*) for metastable decays *via* Eqs (I) (a) and (II) (b) in valine.

The ratios of metastable ions, product ions, and precursor ions $[m^*]/[P^-]$ and $[D^-]/[P^-]$ simulated for reactions (Ia)–(Id) on the basis of the calculated micro-canonical rate constants are shown in Fig. 6. It is most interesting to compare the $[m^*]/[P^-]$ ratios, because, unlike product ions, metastable ions are formed in a rigidly certain time interval (during the drift of ions in the first field-free area of the instrument) and are distinctly related to a specific dissociative process. As can be seen from Fig. 6, reaction (Ib) corresponding to the decomposition of the $[M - H]^-_N$ ions by hydrogen atom migration from position C_α and formation of product ions of the $NH=CCH(CH_3)_2^-$ type demonstrates good agreement with experiment. In the case of processes (Ic) and (Id), there is some discrepancy with the experimental ratio, whereas the experimental and calculated data are quite contradictory for decay (Ia). Inconsistency with experimental data is observed for all calculated curves for the $[D^-]/[P^-]$ ratios. However, unlike metastable ions, prod-

uct ions can be formed due to side migration processes and undergo further decomposition, which is ignored in model calculations.

The structures $COOH^-$ and $HCOO^-$ are possible in decay (II) for product ions with m/z 45. The former can be formed due to the direct bond cleavage in the $[M - H]^-_N$ and $[M - H]^-_{C_\beta}$ ions (reactions (IIa) and (IIb)). Ions with the $HCOO^-$ structure are possible in the case of decay of the $[M - H]^-_O$ ions (reactions (IIc) and (IId)).

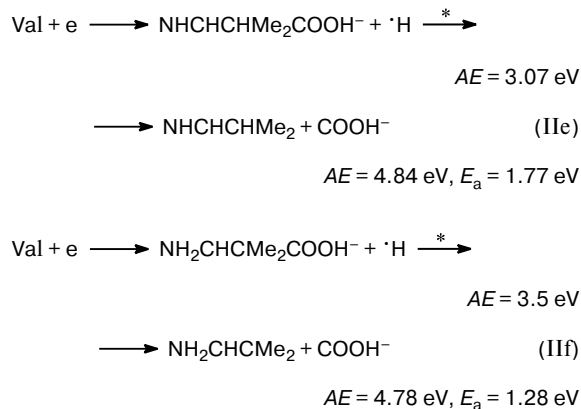




The yield of the COOH^- ions from the $[\text{M} - \text{H}]_{\text{C}\alpha}^-$ ions is accompanied by the formation of a biradical particle and, hence, this decay process was not considered.

We found no experimentally determined published value of electron affinity for the $\cdot\text{COOH}$ particle and, therefore, the value $EA(\cdot\text{COOH}) = 1.51 \text{ eV}$ obtained by the DFT quantum chemical calculations was used for the calculation of the energy characteristics of reactions (IIa) and (IIb). At the same time, the experimental value of electron affinity for similar $\text{HC}\cdot\text{O}$ particle is

$EA = 0.31 \text{ eV}$,²⁴ which asks about a possible overestimation of the calculated $EA(\cdot\text{COOH})$ values. Therefore, we also considered alternative reactions (IIe) and (IIf) for which the value $EA(\cdot\text{COOH}) = 0.31 \text{ eV}$ was used.



As can be seen from Fig. 6, the best agreement with the experimental data is demonstrated by the $[\text{m}^*]/[\text{P}^-]$ curves for reactions (IIe) and (IIf) describing the decay of the $[\text{M} - \text{H}]_{\text{N}}^-$ and $[\text{M} - \text{H}]_{\text{C}\beta}^-$ ions, respectively. Somewhat worse result is demonstrated by the curve for reaction (IIa).

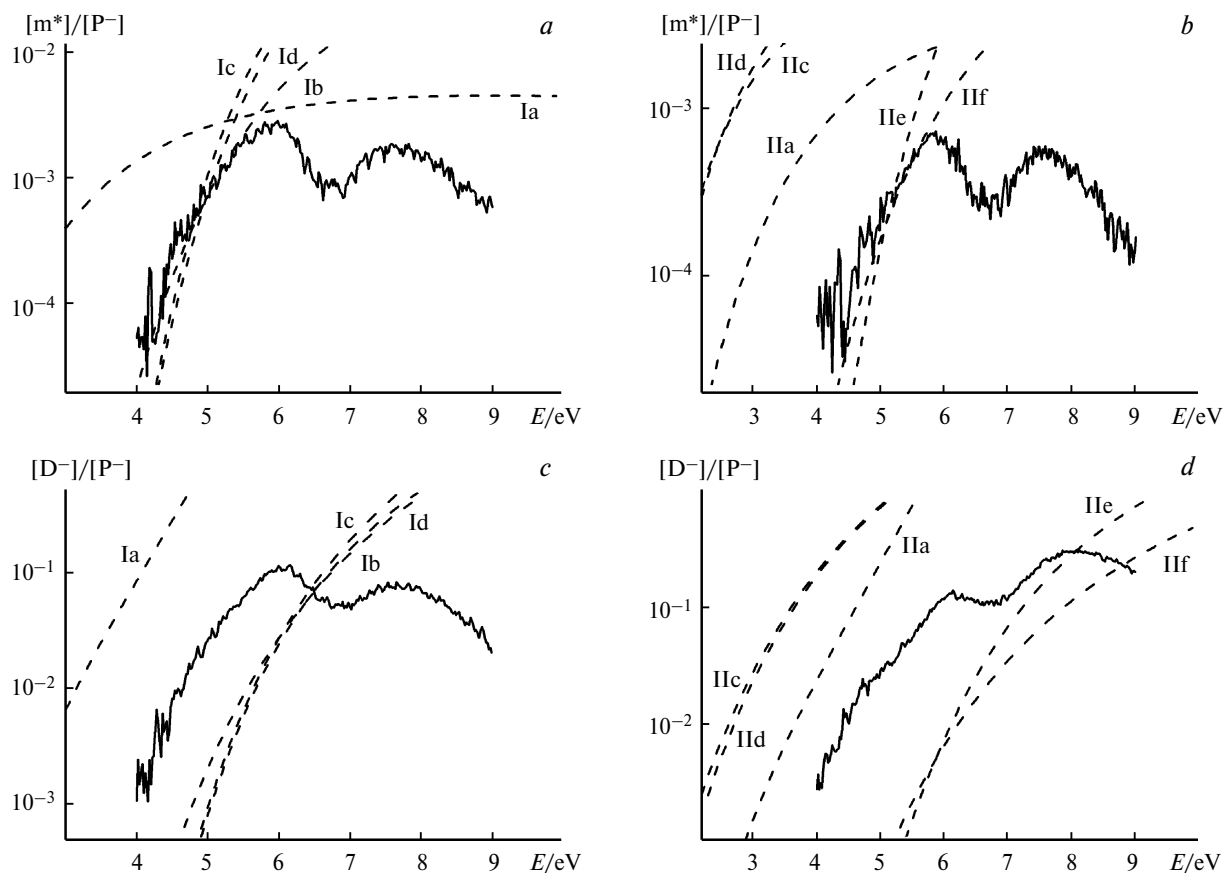


Fig. 6. Experimental (solid lines) and calculated (dashes) ratios $[\text{m}^*]/[\text{P}^-]$ (a, b) and $[\text{D}^-]/[\text{P}^-]$ (c, d) for reactions (I) (a, c) and (II) (b, d) in valine.

Considerable discrepancy with the experimental curve is observed for decays (IIc) and (IId), and the calculated curves for process (IIb) are beyond Fig. 6. Note that in reactions (IIe) and (II f), showing good correspondence with experimental data, the electron affinity for $\cdot\text{COOH}$ was accepted equal to 0.31 eV, which is lower than the calculated value of 1.51 eV. However, a special study is required to clarify this problem, which is beyond the present work.

Resonant electron capture by valine and proline molecules occurs in a wide energy range (0–12 eV) and results in the formation of many negative ions. The obtained mass spectrum of negative valine ions agrees well with the results of previous studies. In the case of proline, earlier undetected low-intensity fragmentation channels were observed. Analogies and distinctions in ion formation processes were observed by a comparative analysis of the mass spectra of resonant electron capture by molecules of both compounds. For instance, the distinctions appear in the absence of $[\text{M} - \text{NH}_2]^-$ and $[\text{M} - \text{NH}_3]^-$ ions in proline and, at the same time, in the appearance of new channels of decay of molecular ions, which are not characteristic of valine and other aliphatic amino acids. A comparative analysis revealed that in the case of proline in the low-energy region the characteristic initial stage of amino acid fragmentation accompanied by the H-shift with the further dissociation of the $\text{N}-\text{C}_\alpha$ bond results in pyrrolidine ring opening and isomerization of the initial geometry of the molecular ion in the configuration $\text{NH}_2\text{CH}_2\text{CH}_2\text{CH}_2\text{CHCOO}^{\cdot-}$ or $\text{NHCH}_2\text{CH}_2\text{CH}_2\text{CH}_2\text{COO}^{\cdot-}$. The new structures of molecular negative ions of proline differ considerably from those for branched amino acids, which results in the formation of other fragment ions. Unlike other earlier studied amino acids, the metastable fragmentation of the $[\text{M} - \text{H}]^-$ ions with the yield of fragment ions CHO_2^- and $[\text{M} - \text{H} - \text{CH}_2\text{O}_2]^-$ was observed in valine and proline. The use of the earlier proposed statistical model for metastable decay suggests that the precursor ions have the imine structure $[\text{M} - \text{H}]^-_{\text{N}}$, and the fragmentation of the $[\text{M} - \text{H}]^-_{\text{C}\beta}$ ions also possibly contributes to decay (II).

This work was financially supported by the Russian Foundation for Basic Research (Project No. 08-03-91101-a) and CRDF (Grant RUC1-2908-UF-07).

References

1. S. Gohlke, A. Rosa, E. Illenberger, F. Brünig, M. A. Huels, *J. Chem. Phys.*, 2002, **116**, 10164.
2. S. Ptasińska, S. Denifl, P. Candori, S. Matejcik, P. Scheier, T. D. Märk, *Chem. Phys. Lett.*, 2005, **403**, 107.
3. P. Papp, J. Urban, S. Matejcik, M. Stano, O. Ingólfsson, *J. Chem. Phys.*, 2006, **125**, 204301.
4. S. Denifl, H. D. Flosadóttir, A. Edtbauer, O. Ingólfsson, T. D. Märk, P. Scheier, *Eur. Phys. J. D*, 2010, **60**, 37.
5. P. Papp, P. Shchukin, S. Matejcik, *J. Chem. Phys.*, 2010, **132**, 014301.
6. J. Kočíšek, P. Papp, P. Mach, Y. V. Vasil'ev, M. L. Deinzer, Š. Matejcik, *J. Phys. Chem. A*, 2010, **114**, 1677.
7. Y. V. Vasil'ev, B. J. Figard, V. G. Voinov, D. F. Barofsky, M. L. Deinzer, *J. Am. Chem. Soc.*, 2006, **128**, 5506.
8. H. Abdoul-Carime, E. Illenberger, *Chem. Phys. Lett.*, 2004, **397**, 309.
9. P. Sulzer, E. Alizadeh, A. Mauracher, T. D. Märk, P. Scheier, *Int. J. Mass Spectrom.*, 2008, **277**, 274.
10. H. Abdoul-Carime, S. Gohlke, E. Illenberger, *Chem. Phys. Lett.*, 2005, **402**, 497.
11. V. A. Mazunov, P. V. Shchukin, R. V. Khatymov, M. V. Muftakhov, *Mass-spektrometriya [Mass Spectrometry]*, 2006, **3**, 11 (in Russian).
12. M. V. Muftakhov, Yu. V. Vasil'ev, V. A. Mazunov, *Rapid Commun. Mass Spectrom.*, 1999, **13**, 1104.
13. R. V. Khatymov, M. V. Muftakhov, V. A. Mazunov, *Rapid Commun. Mass Spectrom.*, 2003, **17**, 2327.
14. J. Wu, X. Xu, *J. Chem. Phys.*, 2007, **127**, 214105.
15. P. V. Shchukin, M. V. Muftakhov, R. V. Khatymov, A. V. Pogulay, *Int. J. Mass Spectrom.*, 2008, **273**, 1.
16. J. C. Lorquet, *Int. J. Mass Spectrom.*, 2000, **200**, 43.
17. A. Pelc, W. Sailer, P. Scheier, M. Probst, N. J. Mason, E. Illenberger, T. D. Märk, *Chem. Phys. Lett.*, 2002, **361**, 277.
18. W. Sailer, A. Pelc, M. Probst, J. Limtrakul, P. Scheier, E. Illenberger, T. D. Märk, *Chem. Phys. Lett.*, 2003, **378**, 250.
19. A. Pelc, W. Sailer, P. Scheier, T. D. Märk, E. Illenberger, *Chem. Phys. Lett.*, 2004, **392**, 465.
20. A. M. Scheer, P. Mozejko, G. A. Gallup, P. D. Burrow, *J. Chem. Phys.*, 2007, **126**, 174301.
21. M. V. Muftakhov, P. V. Shchukin, *Izv. Akad. Nauk, Ser. Khim.*, 2010, 875 [*Russ. Chem. Bull., Int. Ed.*, 2010, **59**, 896].
22. Yu. V. Vasil'ev, B. J. Figard, D. F. Barofsky, M. L. Deinzer, *Int. J. Mass Spectrom.*, 2007, **268**, 106.
23. P. V. Shchukin, M. V. Muftakhov, J. Morré, M. L. Deinzer, Y. V. Vasil'ev, *J. Chem. Phys.*, 2010, **132**, 234306.
24. V. V. Takhistov, D. A. Ponomarev, *Organicheskaya mass-spektrometriya [Organic Mass Spectroscopy]*, Izd-vo VVM, St. Petersburg, 2005, 344 pp. (in Russian).
25. H. D. Flosadóttir, S. Denifl, F. Zappa, N. Wendt, A. Mauracher, A. Bacher, H. Jónsson, T. D. Märk, P. Scheier, O. Ingólfsson, *Angew. Chem., Int. Ed.*, 2007, **46**, 8057.
26. H. G. Flosadóttir, O. Ingólfsson, *J. Phys. Conf. Ser.*, 2008, **115**, 012014.

Received April 6, 2011;
in revised form September 6, 2011